

Monolithically Fabricated 4096-Element, PolyStrata® Broadband D-band Array Demonstrator

Jared Williams Jordan^{*1}, Seth Lynch^{*}, Michael Clark^{*}, Benjamin L. Cannon^{*}, Luis A. Adames^{*}, Darel Wrenn^{*}, Kimberly Jackson^{*}, Neal Erickson^{*}, Justin Clough^{*}, Darryl Brown^{*}, Jean-Marc Rollin^{*},

Pierre Lopez^{#2}, Pascal Boutet[#], Maurizio Moretto[#]

^{*}Nuvotronics, Inc., Durham, NC, USA

[#]Nokia, Paris-Saclay, France

¹jjordan@nuvotronics.com, ²pierre.lopez@nokia.com

Abstract—We present a monolithically fabricated PolyStrata®-based 64x64 array composed of 4096 tightly coupled dipole D-band elements connected by a 4096-way reactive corporate feed network, operating over the 130-175 GHz frequency range. Measured farfield patterns, return loss and realized gain versus simulation are captured. Additionally, we demonstrate the repeatability of the fabrication process by reporting on the performance of multiple smaller 16x16 arrays fabricated on the same mask set. Monolithically fabricated PolyStrata®-based radiators can be an enabler for wafer-level scale arrays which require stable and well-matched input impedance, high efficiency and broadband performance.

Keywords— antenna arrays, broadband antennas, tightly coupled dipole arrays (TCDA), millimeter wave propagation internet of things (IOT), millimeter wave communication

I. INTRODUCTION

With current communication frequency bands becoming more congested with an ever-increasing demand for high-speed data, the commercial industry is pushing communication infrastructures to operate at higher frequencies and with agile and increased instantaneous bandwidths within the millimeter-wave (mmW) spectrum. Aside from the apparent incurred headaches, such as increased atmospheric absorption, challenging sub-system specifications require accurate fabrication and compact packaging techniques which often contradict the ultimate customer needs for low-cost. Traditional low-cost substrate materials are hitting hard upper-frequency usability limits and standard manufacturing processes are restricting the designer in his/her ability to identify a balanced cost-performance solution, let alone their ability to identify the optimum one.

Specifically, D-band, 110-170 GHz, has been identified as one new home for communication traffic [1]-[4] and specifications for key component and sub-systems are being defined. The communication link sub-system responsible for transitioning guided RF energy to free-space, and vice-versa is the antenna. With sub-mil ($<0.001''$) tolerances having an appreciable effect on electrical path lengths, sensitive coupling gaps and substrate thicknesses; bulky machined reflector dishes, horn feeds and RF components have served as the main avenue for hardware implementation.

While dish antennas are tried-and-true, they are often bandwidth limited by a waveguide-based feed and are only capable of limited electronic scanning without suffering from

significant performance degradation. Alternatively, researchers in the field are investigating flat-plate waveguide-based radiator arrays and corporate feed networks [5]. Zhou successfully demonstrates a low-profile, 30 dBi gain antenna across the 130-149 GHz frequency range by stacking and assembling multiple micromachined copper plates [6]. This manufacturing approach leverages the accuracy of photolithographically defined features, however lacks in its ability to define transmission line media other than single conductor waveguides. This limits its ability to achieve wide bandwidths and miniaturization associated with multi-conductor transmission line media like coax.

The next step in the evolution of flat-panel D-band antennas is the incorporation of electronic scanning. It is the focus of this paper to demonstrate the ability to fabricate finely-featured D-band radiating elements on a sub-lambda pitch by utilizing PolyStrata® fabrication technology [7].



Fig. 1. PolyStrata® Fabricated copper tightly coupled dipole array (TCDA) D-band radiators.

II. DESIGN

A primary project goal was to develop and demonstrate a radiating element, leveraging the micron-precision of the PolyStrata® fabrication process, that could be used within a fixed beam antenna and will be expanded upon to enable future electronically steered D-band apertures. This moved the design emphasis more towards implementing an element topology that could reside on a sub-lambda element pitch and less on developing a radiating structure limited to broadside only operation [5].

Baseline with an element pitch of 1.16 mm, corresponding to 0.677 lambda at 175 GHz, paired with the requirement to cover the 130-175 GHz frequency range pushed the PolyStrata® radiator design towards a tightly coupled dipole topology. With limited real-estate below the ground plane, the

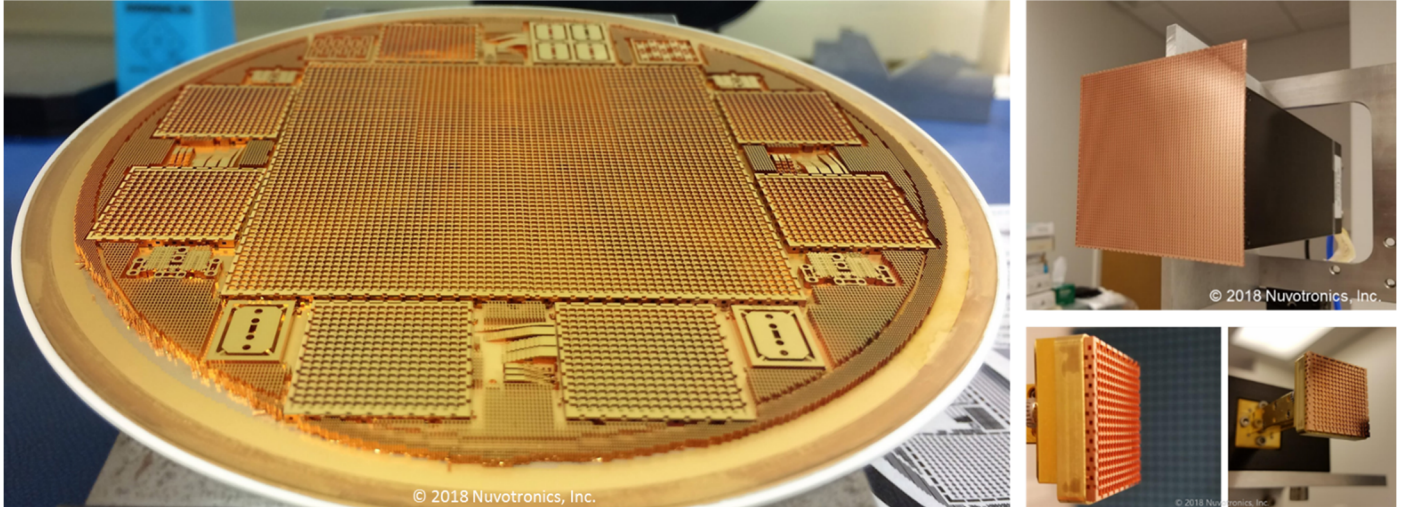


Fig. 2. (left) PolyStrata® Fabricated 6" wafer from Radford, VA facility. (upper right) 4096-element, 64x64 array mounted to PNA frequency extender head. (lower right and middle) 256-element, 16x16 array mounted to PNA frequency extender head.

balun mechanism was incorporated directly with the radiator, above the ground plane [8],[9].

In recent years, there has been significant activity in the arena of pushing broadband arrays into the millimeter-wave frequency regions to simultaneously cover multiple mmW 5G and ISM bands [10] and support wireless connectivity for Internet of Things (IoT) [11]. Novak presents a TCDA design which covers 24-72 GHz and illustrates the challenges of fabricating these radiating structures in traditional PCB fabrication via the comparison of simulated to measurement results for different active elements within a 3x3 array. Sahin presents a monolithically fabricated mmW TCDA array which operates from 35-75 GHz and achieves good simulation to measurement agreement since the array utilizes photolithography to precisely define geometries, like the work presented here. However, SU-8 is used as the main substrate material and the radiation efficiency suffers across the design band (60-80%). Furthermore, an external balun mechanism is still required to drive the radiating element.

While dual-polarization designs with greater bandwidth ($>4:1 F_{high}/F_{low}$) are achievable in PolyStrata® technology [12], emphasis was placed on an all-metal single-polarization radiator design that can cover the 130-175 GHz bandwidth of interest, Fig. 1. The full-wave infinite unit-cell simulation of the radiator predicts 99% radiation efficiency. The only dissipative losses are associated with that of the copper structures which possess a surface roughness of $< 100\text{nm Ra}$.

Broadband reactive H-tree corporate feed networks were implemented behind both the 16x16 and 64x64 array demonstrator designs. The array of radiating elements and the H-tree coaxial feed network are monolithically fabricated together and a secondary piece of PolyStrata® hardware is assembled onto the back where the coaxial feed is transitioned to a WR-6 waveguide. Earlier versions of the demonstrator implemented coaxial-to-waveguide transitions and a H-tree waveguide feed network for the first 8 power splits, greatly reducing the feed network loss. However, the implementation of the waveguide required several additional strata below the

4x4 coaxial feed network and associated TCDA radiators. To expedite the schedule of the program, the waveguide network was removed from both array designs but could be re-incorporated into follow-on efforts if reducing feed network losses is of primary concern.

III. MEASURED AND SIMULATED RESULTS

Two VDI WR6.5-VNAX extender heads and a WR-6 waveguide calibration kit were procured from Virginia Diodes Inc. One extender head was configured for receive only and the other was configured with both transmit and receive functionality. The RX PNA extender head was connected to the SAGE 23 dBi D-band rectangular standard gain horn and was mounted to the back wall, Fig. 3. The TX/RX PNA extender head was mounted on top of the in-house antenna range gimbal and was used to connect to the antenna under test (AUT). The in-house antenna range uses a roll, over elevation over azimuth configuration. Both the roll and elevation are adjusted manually, and the azimuth rotation is automated by a Newport rotation stage. AUT realized gain measurements were performed by the gain substitution method using a second 23 dBi gain horn as the reference antenna.

The measured E/H patterns for a 16x16 array demonstrator can be seen in Fig. 4 and Fig. 5. As one would expect from a



Fig. 3. In-house antenna pattern range utilizing VDI WR6.5-VNAX extender heads and SAGE 23 dBi D-band rectangular standard gain horn.

uniformly illuminated square aperture, the first sidelobe levels are about -13.26 dB and the beamwidth narrows with increasing frequency. The measured gain and theoretical aperture directivity can be seen in Fig. 6 for three individual 256-element arrays. The associated return loss data is captured in Fig. 7. The repeatability of the measured realized gain and return loss performance is excellent. Better than -15 dB return loss is achieved across most of the band and the total efficiency of the 256-element array and feed network is better than 70%.

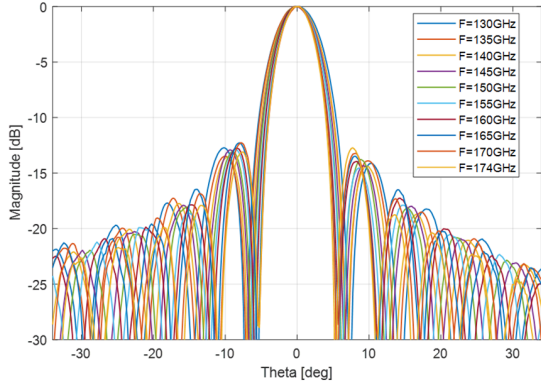


Fig. 4. Measured E-plane patterns for 256-element, 16x16 array.

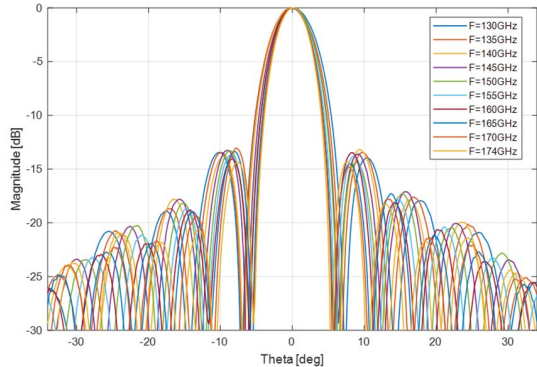


Fig. 5. Measured H-plane patterns for 256-element, 16x16 array.

One 64x64 array demonstrator can be fabricated in the center of a single 6" wafer, Fig. 2. The measured E/H-plane patterns of one 4096-element demonstrator can be seen in Fig. 8 and Fig. 9. The $2^*D^2/\lambda$ farfield distance limit is 42 feet, using the array diagonal as D and lambda calculated at 175 GHz [13]. The radiation characteristics reported here are measured at 15 feet between the antenna range horn and AUT. The impact of measuring at a closer distance degrades the measured gain slightly (few tenths to half of a dB) and increases the sidelobe levels by 1-2 dB. This impact to gain and sidelobe levels was confirmed with the use of an array code where the free-space green's function observation radius was simulated as finite, rather than using a farfield assumption [13]. The measured realized gain and theoretical aperture directivity can be seen in Fig. 10 and the associated return loss for the 4096-element array is captured in Fig. 11. As was stated previously, the total efficiency of 30% or greater across the band could be greatly improved by replacing the first 8 reactive splits with a waveguide combiner network at the extra cost and schedule of fabricating additional strata underneath the 4x4 sub-array coaxial sub-array corporate feed.

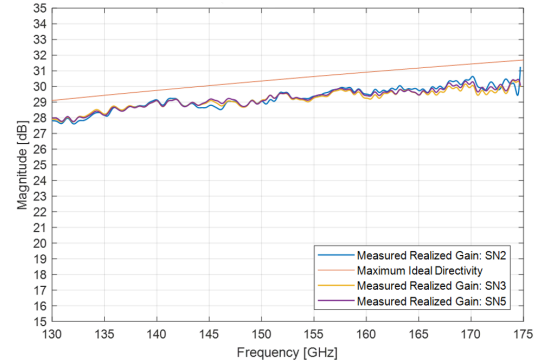


Fig. 6. Measured realized gain for quantity 3, 256-element, 16x16 arrays plotted along with maximum ideal directivity associated with an 18.56 mm square aperture.

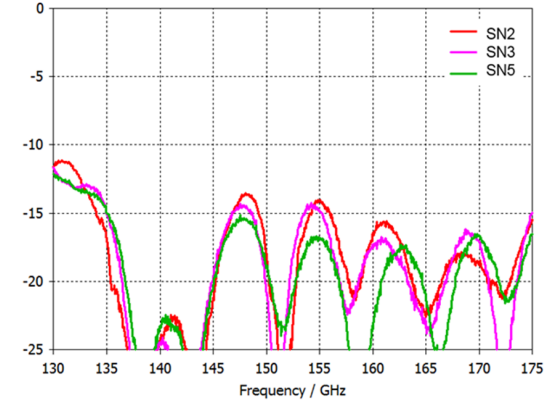


Fig. 7. Measured return loss (dB) for quantity 3, 256-element, 16x16 arrays.

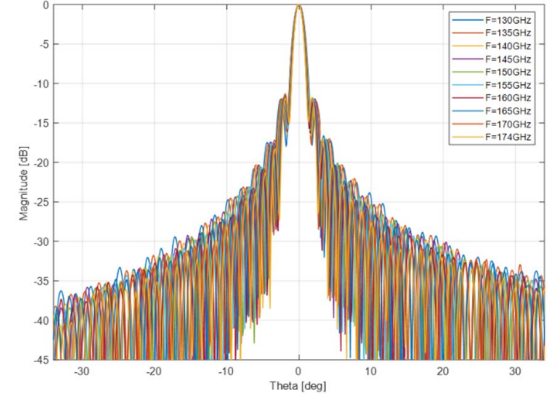


Fig. 8. Measured E-plane patterns for the 4096-element, 64x64 array.

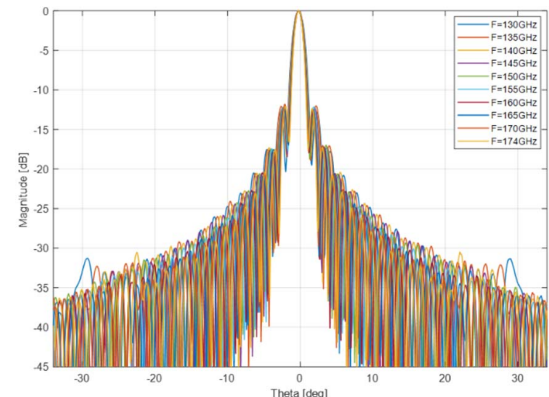


Fig. 9. Measured H-plane patterns for the 4096-element, 64x64 array.

The correlation between measured and simulated realized gain is excellent and is important for a couple of reasons. First, it further validates our design/modelling techniques at these millimeter frequencies. Second, it validates the monolithic fabrication of these very large element count arrays, fed entirely by reactive combiners. Often, traditional arrays are fed by corporate feed networks utilizing resistive elements to implement output isolation. This is instantiated to compensate for fabrication errors present in traditional manufacturing techniques (PCB, machining, 3-D printing, etc.). Other than a moderate level of measured realized gain ripple, significant gain drop-outs or increasing return-loss are not witnessed across the entire 130-175 GHz frequency range of interest. It is important to note that implementing reactive corporate feed networks with larger bandwidths ($>4:1 F_{high}/F_{low}$) is achievable by the incorporation of additional quarter-wavelength transformers.

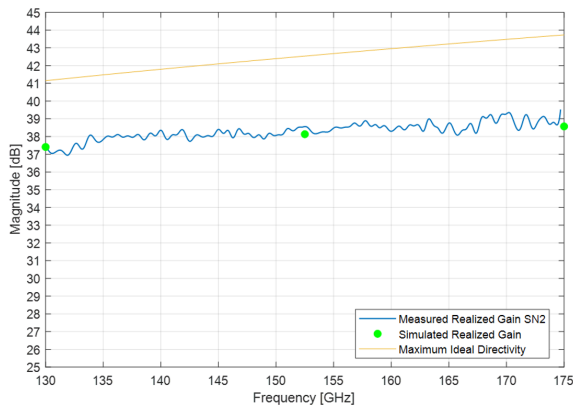


Fig. 10. Measured realized gain for 4096-element, 64x64 array plotted along with maximum ideal directivity associated with a 74.24 mm square aperture. Simulated realized gain results from a fullwave simulation of the entire array and feed network are marked by green circles.

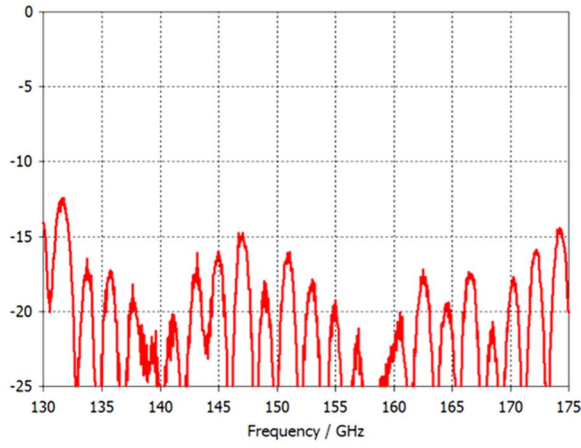


Fig. 11. Measured return loss (dB) for the 4096-element, 64x64 array.

IV. CONCLUSIONS

To the best of our knowledge, we have demonstrated the largest D-band array (4096 elements), where individual radiators reside on less than a lambda pitch and are fed from a common feed point (WR-6). The all-copper tightly coupled dipole array radiator was designed to operate across the 130-

175 GHz frequency band of interest and possesses 99% radiation efficiency. The radiators and reactive H-tree combiners were fabricated together as one monolithic part, utilizing the PolyStrata® fabrication process, and excellent part-to-part repeatability was demonstrated. Common issues associated with reactive corporate feed networks fabricated with traditional processes, often manifest themselves as significant gain drop-outs versus frequency and no such issues are present in the data reported here.

Monolithically fabricated PolyStrata®-based radiators can be an enabler for wafer-level scale arrays which require stable and well-matched input impedance, high efficiency and broadband performance.

ACKNOWLEDGMENTS

The authors acknowledge the continued advancements by the Nuvotonics fabrication, assembly and engineering teams.

REFERENCES

- [1] S. Carpenter, Z. He, M. Bao and H. Zirath, "A Highly Integrated Chipset for 40 Gbps Wireless D-Band Communication Based on a 250 nm InP DHBT Technology," *2014 IEEE Compound Semiconductor Integrated Circuit Symposium (CSICS)*, La Jolla, CA, 2014, pp. 1-4.
- [2] D. Hou *et al.*, "D-band on-chip higher-order-mode dielectric-resonator antennas fed by half-mode cavity in CMOS technology," in *IEEE Antennas and Propagation Magazine*, vol. 56, no. 3, pp. 80-89, June 2014.
- [3] S. Beer *et al.*, "Design and measurement of matched wire bond and flip chip interconnects for D-band system-in-package applications," *2011 IEEE MTT-S International Microwave Symposium*, Baltimore, MD, 2011, pp. 1-4.
- [4] B. Göttel, S. Beer, M. Pauli and T. Zwick, "Ultra wideband D-band antenna integrated in a LTCC based QFN package using a flip-chip interconnect," *2013 European Microwave Conference*, Nuremberg, 2013, pp.227-230.doi: 10.23919/EuMC.2013.6686632
- [5] M. M. Zhou and Y. J. Cheng, "D-Band High-Gain Circular-Polarized Plate Array Antenna," in *IEEE Transactions on Antennas and Propagation*, vol. 66, no. 3, pp. 1280-1287, March 2018.
- [6] L. Chang, Z. Zhang, Y. Li, S. Wang and Z. Feng, "60-GHz Air Substrate Leaky-Wave Antenna Based on MEMS Micromachining Technology," in *IEEE Transactions on Components, Packaging and Manufacturing Technology*, vol. 6, no. 11, pp. 1656-1662, Nov. 2016.
- [7] D. S. Filipovic, Z. Popovic, K. Vanhille, M. Lukic, S. Rondineau, M. Buck, G. Potvin, D. Fontaine, C. Nichols, D. Sherrer, S. Zhou, W. Houck, D. Fleming, E. Daniel, W. Wilkins, V. Sokolov, and J. Evans, "Modeling, Design, Fabrication, and Performance of Rectangular-Coaxial Lines and Components", *2006 IEEE MTT-S International Microwave Symposium Digest*, San Francisco, CA, pp 1393-1396.
- [8] S. S. Holland and M. N. Vouvakis, "The Planar Ultrawideband Modular Antenna (PUMA) Array," in *IEEE Transactions on Antennas and Propagation*, vol. 60, no. 1, pp. 130-140, Jan. 2012.
- [9] J. P. Doane, W. F. Moulder, K. Sertel and J. L. Volakis, "Wideband, wide scanning conformal arrays with practical integrated feeds," *2013 International Symposium on Electromagnetic Theory*, Hiroshima, 2013, pp. 859-862.
- [10] Novak, Markus. *Low Cost Ultra-Wideband Millimeter-Wave Phased Arrays*. Diss. The Ohio State University, 2017.
- [11] S. Sahin, N. K. Nahar and K. Sertel, "Performance Characterization of Monolithically Integrated mmW Phased Arrays." *2018 IEEE International Symposium on Antennas and Propagation and USNC-URSI Radio Science Meeting*, Boston, 2018.
- [12] J. W. Jordan *et al.*, "PolyStrata® X/Ku/Ka-band, Dual-Polarized, Tightly Coupled Dipole Scannable Focal Plane Array" *2018 IEEE International Symposium on Antennas and Propagation and USNC-URSI Radio Science Meeting*, Boston, 2018.
- [13] Constantine, A. Balanis. "Antenna theory: analysis and design." *third edition*, John wiley & sons (2005).